

## HiSST: 4th International Conference on High-Speed Vehicle Science Technology 22 -26 September 2025, Tours, France



# Investigation of different skin friction coefficient calculation methods applicable to the design of hypersonic vehicles using MDAO approaches

Paul Russell LANCRY<sup>1</sup>, Romain WUILBERCQ<sup>2</sup> DTIS, ONERA Université Paris-Saclay, 91120 Palaiseau-France

#### **Abstract**

This article investigates the validity of different computational methodologies that lead to reliable estimates of skin friction coefficients. The approaches considered are readily applicable in the context of Multidisciplinary Design Analysis and Optimization (MDAO) during the conceptual design phases of hypersonic vehicles. Moreover, the computational expense associated with these methods remains minimal, thereby rendering them particularly suitable for iterative applications in preliminary design optimization frameworks. These computations were conducted utilizing the in-house tool SHAMAN, developed at ONERA, which will be briefly presented herein. In particular, reference temperature (or more broadly enthalpy) models are evaluated alongside established methodologies such as the Van Driest II and Spalding & Chi methods. The present work sets up a series of benchmark test cases derived from data reported in the open scientific literature, and aims to propose a hierarchy of computational methods for the estimation of vehicle skin friction coefficient distributions in the context of conceptual design phases. The validity of each method is determined through comparison of its numerical predictions with corresponding experimental data. Based on these comparisons, a ranking of methods is established according to their accuracy and genericity in replicating empirical results. In particular, three different sets of test cases are explored: flat plates at zero incidence without pressure gradients, flat plates at nonzero incidence values and plates with blunt leading edges, all immersed in hypersonic freestream conditions. Moreover, the paper presents a systematic procedure to establish a reference temperature formulation based on available data. Finally, the article illustrates how these methods can be used in an MDAO study on an ONERA hypersonic vehicle named 'JAPHAR'. This article provides an initial methodological framework for the calculation of skin friction coefficients, intended to support practitioners and researchers involved in hypersonic vehicle design, using MDAO or systems engineering approaches.

Keywords: Hypersonic Vehicle Design, Skin Friction Coefficients, Reference Temperatures

#### **Nomenclature**

P - Pressure

R<sub>e</sub>- Reynolds Number

T - Temperature

Pr - Prandtl number

M – Mach Number

h – Specific Enthalpy

V - Velocity

 $C_p$  – Heat Capacity

 $\rho$  – Density

<sup>&</sup>lt;sup>1</sup> Systems Engineer, ONERA, paul.lancry@onera.fr

<sup>&</sup>lt;sup>2</sup> Systems Engineer, ONERA, romain.wuilbercq@onera.fr

 $C_f$  – Compressible Skin friction coefficient

 $C_{f,INC}$  – Incompressible Skin Friction Coefficient

Subscripts

e – At the edge of the boundary Layer

w - At the wall

f - Adiabatic wall

x – distance of the centroid of the element from the nose of the leading edge

#### 1. Introduction

The design phase of airbreathing hypersonic vehicles is a highly complex and is an inherently iterative process, driven by demanding and often competing performance requirements. In particular, such vehicles must demonstrate the capability to operate across a broad range of high Mach numbers within multiple layers of the atmosphere while fulfilling their prescribed mission objectives. Consequently, during their missions, such vehicles are exposed to harsh aerodynamic heating and high-pressure environments, resulting in complex multi-physical interactions [1]. The multi-disciplinary nature of these interactions has motivated the adoption of Multi-Disciplinary Design Analysis and Optimization (MDAO) for their design. MDAO leverages numerical optimization techniques to solve problems involving tightly coupled disciplines. Due to the complexity inherent in multidisciplinary coupling, designers frequently restrict the use of high-fidelity computational tools to better manage computational resource requirements.

This paper examines methodologies for estimating the skin friction coefficient of hypersonic vehicles. In particular, computationally efficient methods are discussed. The study of skin friction is essential, as it enables designers to estimate the skin friction drag component of a vehicle's total drag. This estimation is particularly important when evaluating propulsive requirements and/or thermal protection systems during conceptual design phases or within MDAO frameworks.

This paper is organized into four main sections. First, the in-house software SHAMAN and the different employed computational methods are introduced. Second, a validation procedure is proposed and applied to three test case databases built from reference literature data. Third, a procedure is proposed for calibrating a reference temperature model using a user-defined dataset. Finally, SHAMAN's ability to apply such methods within an 'MDAO-like' approach will be illustrated on the ONERA hypersonic vehicle JAPHAR [14].

#### 2. Presentation of the Software and Methodologies Considered

#### **2.1. SHAMAN**

The primary tool used in this work is SHAMAN, a Python-based software developed in-house at ONERA. SHAMAN can be employed to predict the aero-thermodynamic environment of supersonic and hypersonic vehicles during conceptual design phases. It incorporates a series of well-established analytical and semi-empirical approaches referred to as Local Surface Inclination (LSI) methods [15]. including the classical and modified Newtonian Theory, as well as the Tangent-Wedge and Tangent-Cone models. These methods require a triangulated mesh representation of the vehicle geometry, the local inclination angles of all surface panels, and the freestream conditions as inputs. These LSI methods are employed to compute the inviscid aerodynamic environment, providing rapid estimates of surface pressure distributions and boundary layer edge conditions, necessary to apply the methods described in this work in the context of preliminary design analyses. While the panel-based nature of this approach entails a reduction in physical fidelity compared to modern numerical techniques such as Computational Fluid Dynamics (CFD), its markedly lower computational cost and high parametric flexibility renders it highly effective for many practical applications in conceptual design phases. Indeed, SHAMAN was built from the outset to enable seamless integration into multidisciplinary, multi-fidelity design and optimization frameworks for conceptual design studies. This capability will be further detailed in the following sections of this article.

SHAMAN provides several methods for the computation of skin friction coefficients as a means to account for viscous loads, including those based on the reference temperature models. The following subsections briefly describes these methods most relevant to this study.

#### 2.2. Reference Temperature Method

A significant temperature gradient can develop across the thickness of the boundary layer (BL) on a vehicle's surface during hypersonic flight. By selecting an appropriate representative average (or reference) temperature within the boundary layer, correlations originally formulated for incompressible flow can be extended to the compressible regime. The reference temperature method - sometimes referred to as the 'SOMMER and SHORT' approach [16] — enables the estimation of local flow properties, such as the compressible skin friction coefficient values  $C_f$ , by applying standard incompressible-flow correlations (e.g., the laminar Blasius solution [7] or turbulent van Driest II—type transformations [8]) with fluid properties evaluated at a so-called reference state, typically defined by a 'reference temperature' denoted T\*, or, alternatively, a 'reference enthalpy' (h\*). This reference state is computed as a weighted combination of the boundary-layer edge and wall conditions, thereby enabling the estimation of  $C_f$  under true compressible flow scenarios, through the following relationship [16]:

$$\frac{C_f}{C_f *} = \frac{T_e}{T *} = \frac{\rho *}{\rho_e}$$
 (1)

These techniques provide reasonable accuracy (compared to full-boundary layer solutions) while substantially reducing computational complexity. The latter makes this approach particularly suitable for the rapid assessment of hypersonic vehicles during conceptual designs. From the established reference state, a reference Reynolds Number can be estimated, which can be used to compute the associated reference skin friction coefficient [9] using traditional formulas, linking Reynolds numbers and Skin friction coefficients through relationships of the following form (see also equation 5):

$$C_f *= f(R_{e,x} *) \quad (2)$$

In the `SOMMER and SHORT' method, the reference temperature is defined as a weighted sum of the wall and BL edge temperatures, following the approach originally proposed by Rubesin and Johnson [16]. The empirical coefficients in this formulation were established based on limited experimental data for laminar BLs:

$$\frac{T^*}{T_e} = 1 + 0.035M_e^2 + 0.45\left(\frac{T_w}{T_e} - 1\right) \quad (3)$$

In practical application, local thermodynamic properties such as reference density  $\rho^*$ , reference dynamic viscosity  $\mu^*$  and local Reynolds numbers  $Re_x^*$  are evaluated at the reference temperature. The static pressure is taken from the inviscid LSI methods discussed previously. This approach is justified by the boundary layer approximation, which assumes that the pressure remains nearly constant in the direction normal to the surface across the boundary layer. These assumptions yield the following relationships:

$$\frac{R_{\rm ex}^*}{R_{\rm ex}} = \frac{T_{\rm e}}{T^*} \frac{\mu_{\rm e}}{\mu^*} \quad (3) , \quad \frac{\rho^*}{\rho_{\rm e}} = \frac{T_{\rm e}}{T^*} \quad (4)$$

From this reference state, the compressible skin friction coefficient  $C_f^*$  can then be estimated using well-established formulas such as Prandtl's formulation for skin friction, which may be used typically to give a simple estimate of the viscous drag on thin airfoils or other streamlined shapes like flat plates for a broad range of Reynolds Numbers (up to  $Re_x \sim 10^9$ ) [10]:

$$C_{\rm f}^* = \frac{0.027}{R_{\rm e,x}^{*\frac{1}{7}}} \quad (5)$$

HiSST-2025-0194 Page |3
Investigation of different skin friction coefficient calculation methods applicable to the design of hypersonic vehicles using
MDAO approaches Copyright © 2025 by author(s)

The ratio  $\frac{T*}{T_e}$  is fundamental in enabling the application of incompressible-flow correlations to compressible formulas. Over the years, various expressions for  $\frac{T*}{T_e}$  have been proposed in the literature, each derived from experimental observations and calibrated to address different test cases.

In 1955, Eckert proposed a corrected formula to better fit flat plates with no pressure gradient conditions, for both laminar and turbulent boundary layers [2]. The specific enthalpy expression h\* according to Eckert can be written as:

$$h^* = 0.5 \times (h_e + h_w) + 0.22 \times (h_f - h_e)$$

The former expression may be written in terms of a reference temperature T\* or a ratio between the reference temperature and the boundary layer edge temperature:

$$\frac{T^*}{T_e} = 1 + 0.5 \left( \frac{T_w}{T_e} - 1 \right) + 0.22 \times R_f \times \frac{\gamma - 1}{2} \times M_e^2 \quad (6)$$

Moreover, Monaghan's formula **[12]** also considers the thermal effects on an isothermal wall as well as the adiabatic ones through the use of a recovery factor  $R_f$ , but with a smaller importance in comparison to Eckert's formula. The Monaghan formula is then written as:

$$\frac{T^*}{T_e} = 1 + 0.54 \times \left(\frac{T_w}{T_e} - 1\right) + 0.16 \times R_f \times \frac{\gamma - 1}{2} \times M_e^2 \quad (7)$$

In 1992, Poll suggested its own adjusted formula, but this time for an infinite swept cylindrical leading edge [11]:

$$\frac{T^*}{T_e} = 1 + 0.1 \left( \frac{T_w}{T_e} - 1 \right) + 0.6 \times R_f \times \frac{\gamma - 1}{2} \times M_e^2 \quad (8)$$

Unlike the Eckert and Monaghan formulas which were established on flat plates without pressure gradients ( $u_e = constant$  at the stagnation point), the Poll formula was established on a cylindrical leading edge and yields the most weight to the recovery terms than any other formula.

In 2005, Smart and Meador [17] proposed their own formulas distinguishing both laminar and turbulent boundary layers. For the study of laminar boundary layers, they suggested the following formula:

$$\frac{T*}{T_e} = 0.45 + 0.55 \times \frac{T_w}{T_e} + 0.16 \times R_f \left[ \frac{\gamma - 1}{2} \right] M_e^2 \quad (9)$$

For the study of turbulent boundary layers:

$$\frac{T*}{T_e} = 0.5 \times \left(\frac{T_w}{T_e} + 1\right) + 0.16 \times R_f \left[\frac{\gamma - 1}{2}\right] M_e^2 \quad (10)$$

The purpose of the work presented in **[17]** by Smart and Meador was to propose an alternative definition of what the reference enthalpy is. Indeed, the authors proposed a 'simple average' of the local enthalpy over the velocity profile as the correct definition of the reference enthalpy. Then, by substituting the generalized enthalpy profiles obtained from boundary layer solutions for air-like gases where  $P_r \sim 0.7$  (like those studied in the upcoming validation efforts), equations 9 and 10 were derived by the authors. In particular, for Turbulent boundary layers, the authors used Whitfield and High's first order theory that proposes an expression of the Reynolds stress, to develop an expression of h\* assuming the Reynolds stress to be proportional to the local turbulent kinetic energy. This approach is different from other approaches like that of Eckert who achieved his factors by matching empirically

the reference enthalpy 'corrected' for an incompressible flat plate with a database of solutions of the laminar compressible boundary layer equations by Van Driest.

#### 2.3. Van Driest II Method

The Van Driest II method [8] may be understood as a transformation method: an incompressible formula relating to the skin friction coefficient and the Reynolds number is chosen, then differentiated in order to obtain a relationship between both the local and average skin friction coefficient. Indeed, the Schoenherr formula for the average skin friction coefficient  $(\overline{C_f})$  [12] gives us a representation for incompressible scenarios for a range of Reynold numbers  $R_{e,x} \sim 3 \times 10^5 to 4.5 \times 10^8$ :

$$\frac{0.242}{\sqrt{\overline{C_{f,INC}}}} = log_{10} \left( R_{e,x,INC} \times \overline{C_{f,INC}} \right) \quad (11)$$

$$C_{f,INC} = \frac{0.242 \times \overline{C_{f,INC}}}{0.242 + 0.8686 \times \sqrt{\overline{C_{f,INC}}}}$$
(12)

Using the previous equations, the following transformations are used to determine the skin friction for a compressible boundary layer flow:

$$\overline{C_{f,INC}} = \frac{2 \times R_{e,\theta,INC}}{R_{e,x,INC}}$$

$$C_{f,INC} = F_c \times C_f \quad \& \quad \overline{C_{f,INC}} = F_c \times \overline{C_f}$$

Where  $F_c$ ,  $R_{e,\theta,INC}$  and  $R_{e,x,INC}$  are defined as in [8] at pages 2 and 3.

#### 2.4. Spalding & Chi Method

The Spalding & Chi method described in [3] is very similar to reference temperature-based methods. Indeed, the core idea is to adjust the value of the incompressible skin friction coefficient  $C_{f,INC}$  through an adjusting factor  $F_{INC}$  in order to obtain the true compressible skin friction coefficient:

$$C_f = \frac{1}{F_{INC}} \times C_{f,INC}$$

$$F_{INC} = \frac{\frac{T_f}{T_e} - 1}{\left(sin^{-1}(\kappa) + sin^{-1}(\nu)\right)^2}$$

$$\kappa = \frac{\frac{T_f}{T_e} + \frac{T_w}{T_e} - 2}{\sqrt{\left(\frac{T_f}{T_e} + \frac{T_w}{T_e}\right)^2 - 4 \times \frac{T_w}{T_e}}}$$

$$\nu = \frac{\frac{T_f}{T_e} - \frac{T_w}{T_e}}{\sqrt{\left(\frac{T_f}{T_e} + \frac{T_w}{T_e}\right)^2 - 4 \times \frac{T_w}{T_e}}}$$

HiSST-2025-0194 Page |5 Investigation of different skin friction coefficient calculation methods applicable to the design of hypersonic vehicles using

#### 3. Validation Procedure Based on Literature Data

In the following sections, three separate databases will be assembled from published reference data. Using those, the skin friction coefficient values predicted by each of the previously described methods will be calculated and systematically compared to the reference data. For each method under consideration, the mean relative error will be calculated as follows:

$$\Delta[\%] = 100 \times \langle \frac{\left| C_{f,DATA} - C_{f,COMPUTED} \right|}{C_{f,DATA}} \rangle$$

where the bracket (.) denote averaging over all data points in the database. This metric quantifies the relative deviation between estimated and experimental skin friction coefficients.

## 3.1. Test Case 1: Hypersonic Sharp Flat Plate at Zero Angle of Attack

The first test case considered is the canonical flat plate at zero incidence, with no pressure gradient, subjected to hypersonic flow conditions. A database comprising 281 points was compiled from three independent literature sources [3-4-5] for correlation studies on sharp flat plates without pressure gradients. For each data point, the conditions at the edge of the boundary layer – including temperature, pressure, Reynolds number, and Mach number - are provided, along with the corresponding wall temperature, thereby allowing us to apply the reference temperature-based methods. According to the cited sources, all reference cases pertain to fully turbulent boundary layers.

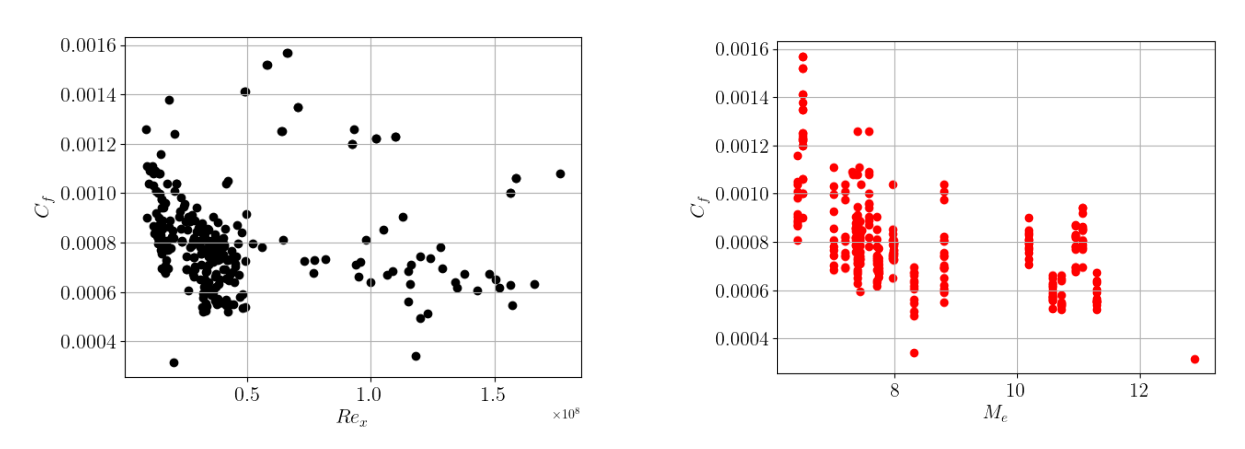


Fig 1. Studied points for Test case scenario 1 [3,4,5]

Moreover, to provide additional information about the data points, the ratio of wall to recovery temperature, noted  $\frac{T_w}{T_f}$ , is also evaluated. This ratio indicates the direction and magnitude of heat flux at the wall: a wall temperature greater than the recovery temperature corresponds to heat flux into the flow, while a lower wall temperature indicates a heat flux into the wall. For this dataset of study, all cases involve ratio values where  $\frac{T_w}{T_f} < 1$ .

For the correlation presented herein, Prandtl's formula will be employed to compute the incompressible skin friction coefficients as it is valid over a broad range of Reynold numbers (typically  $5 \times 10^5$  to  $10^9$ ) [10]. The compressible skin friction coefficient will subsequently be estimated using the reference

temperature-based methods described above and the reference skin friction coefficient computed using equation (5):

| Van<br>Driest II | Spalding<br>& Chi | Smart-<br>Meador | Eckert         | Monaghan           | Poll                   |
|------------------|-------------------|------------------|----------------|--------------------|------------------------|
|                  |                   |                  |                |                    |                        |
| 73.02            | 26.00             | 24.39            | 19.65          | 24.90              | 97.43                  |
|                  |                   |                  |                |                    |                        |
| 89.43            | 60.31             | 80.2             | 105            | 84.1               | 214                    |
| 47.67            | 0.1               | 0.05             | 0.1            | 0.2                | 0.5                    |
| 73.93            | 24.95             | 23.10            | 13.5           | 23.13              | 87.69                  |
|                  | 47.67             | 47.67 0.1        | 47.67 0.1 0.05 | 47.67 0.1 0.05 0.1 | 47.67 0.1 0.05 0.1 0.2 |

**Table 1.** Average mean relative errors for the test case scenario 1

As summarized in Table 1, Poll's formula yields the highest mean relative errors amongst the methods evaluated in the present study. This outcome was predictable: Poll's formula was originally calibrated for cylindrical geometries, and as such, it is not directly applicable to sharp flat plates. In contrast, all other reference temperature-based methods, as well as the Spalding & Chi method, demonstrate superior accuracy compared to the Van Driest II computations for this dataset. While Monaghan's, Smart-Meador's and Spalding & Chi's computation average around 25-26% relative errors, Eckert achieves the lowest average error, at around 20%.

#### 3.2. Test Case 2: hypersonic sharp flat plates at non-zero-incidences

The second test case scenario focuses on sharp flat plates with non-zero incidence angles (non-zero pressure gradients). For this test case, a data sample of 20 points is constructed based on **[3]**. All points are at  $M_{\infty} = 7.4$  for freestream conditions with incidences varying from  $+3^{\circ}$  to  $+6.5^{\circ}$ .

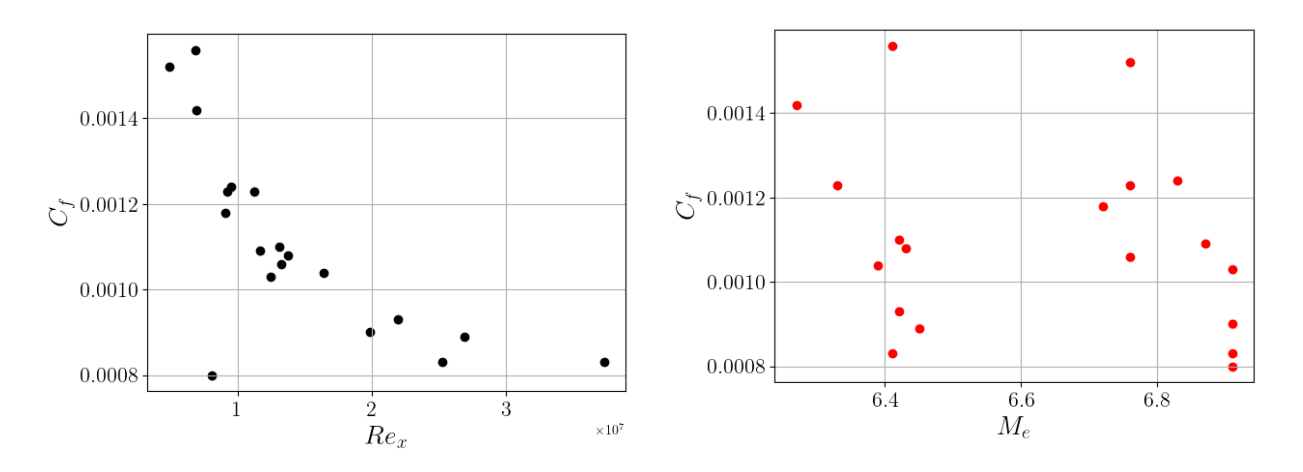


Fig 2. Studied points for test case scenario 2 [3]

This time, we will compare the reference temperature-based models with the analytical model found in **[16]**, which is tailored for flat plates in supersonic freestream conditions for  $5^{\circ} \le \alpha \le 50^{\circ}$  and  $3050 \frac{m}{s} \le V_{\infty} \le 8000 \frac{m}{s}$ :

$$C_f = \frac{1}{R_e^{0.2}} \times \left( 0.048 \sin(4.5\alpha) + 0.7 \frac{V_\infty}{3050} \cos(\alpha)^{2.25} \sin(\alpha)^{1.5} \right)$$
 (14)

HiSST-2025-0194 Page |7
Investigation of different skin friction coefficient calculation methods applicable to the design of hypersonic vehicles using
MDAO approaches Copyright © 2025 by author(s)

A first comparison is made considering points from all incidences yielding the following results:

|            | Analytical<br>Model<br>(Eq 14) | Smart-<br>Meador | Eckert | Monaghan | Poll   |
|------------|--------------------------------|------------------|--------|----------|--------|
| Δ [%]      | 49.7                           | 18.16            | 30.58  | 17.89    | 71.13  |
| Max [%]    | 126.25                         | 39.45            | 38.85  | 39.02    | 115.10 |
| Min [%]    | 2.7                            | 0.10             | 9.60   | 0.2      | 23.45  |
| Median [%] | 28.86                          | 17.86            | 31.08  | 17.82    | 69.10  |

**Table 2.** Average mean relative errors for test case scenario 2 considering all incidences

A second comparison is made considering only the 9 points of the data sample which have incidences above 5°, which fit in equation (14)'s definition field:

|            | Analytical<br>Model | Smart-<br>Meador | Eckert | Monaghan | Poll   |  |
|------------|---------------------|------------------|--------|----------|--------|--|
|            | (Eq 14)             |                  |        |          |        |  |
| Δ [%]      | 11.06               | 18.50            | 30.54  | 18.26    | 69.42  |  |
| Max [%]    | 15.75               | 26.14            | 37.40  | 25.60    | 115.10 |  |
| Min [%]    | 2.7                 | 0.10             | 16.08  | 0.2      | 44.95  |  |
| Median [%] | 14.08               | 22.24            | 32.32  | 22.21    | 64.16  |  |

**Table 3.** Average mean relative errors for test case scenario 2 considering incidences above 5°

In both case cases, Poll's formula performs the worst due to the reason mentioned earlier in test case scenario 1. However, in the first case, when considering both points below and above 5° incidence angles, the Smart-Meador and Monaghan formulas outperform both the analytical model and Eckert's formula, while in the second case, the analytical model vastly outperforms all reference temperature-based methods with an average mean error of merely 11%.

## 3.3. Test Case 3: Hypersonic Plates with Blunt Edges

Test case scenario 3 focuses on hypersonic plates that have blunt edges. Based on **[6]**, a data sample of 59 points is built where the authors studied flat plates in hypersonic freestream conditions at  $M_{\infty}=6.8$ , for varying edge bluntness's defined by a width parameter "t". Only points that correspond to a situation where the boundary layer has transitioned to turbulent are considered.

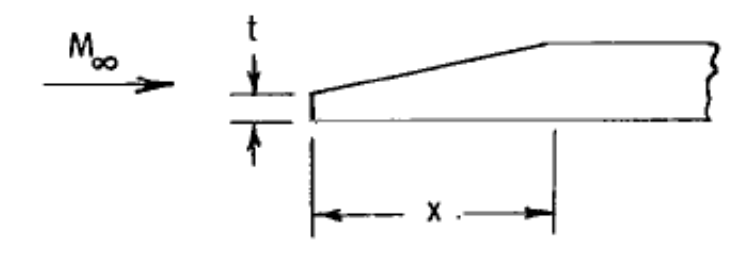


Fig 3. Studied configuration by the authors of [6] (Side-plate)

Two values of bluntness 't' are considered: 0.0025 cm ("sharp configuration") and 1.27 cm ("blunt configuration").

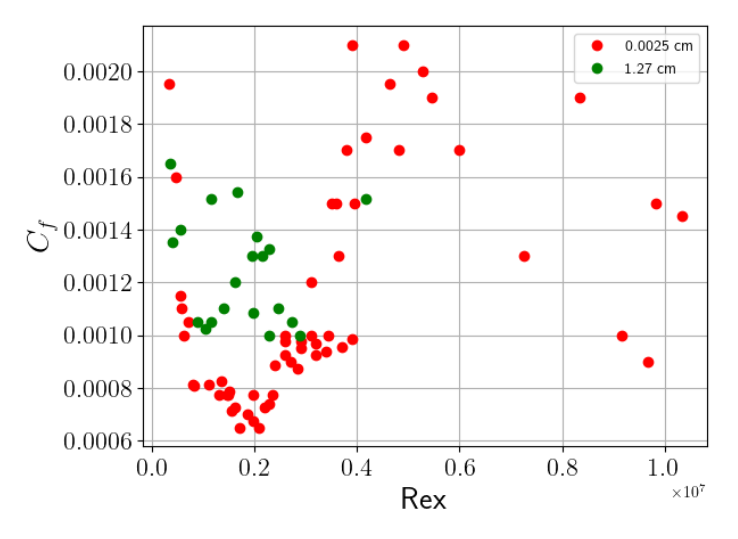


Fig 4. Studied Points for test case scenario 3 (as functions of Reynolds) [6]

A comparison of the different methods yields the following results:

|                 | Van<br>Driest<br>II | Spalding<br>& Chi | Smart-<br>Meador | Eckert | Monaghan | Poll   |
|-----------------|---------------------|-------------------|------------------|--------|----------|--------|
| Δ               | 61.83               | 38.37             | 36.84            | 38.57  | 37.09    | 54.87  |
| @t=0.0025cm [%] |                     |                   |                  |        |          |        |
| Max             | 78.33               | 64.76             | 107              | 131.08 | 112.73   | 192.29 |
| @t=0.0025cm [%] |                     |                   |                  |        |          |        |
| Min             | 30.00               | 1.05              | 2.29             | 0.4    | 0.5      | 2.91   |
| @t=0.0025cm [%] |                     |                   |                  |        |          |        |
| Median          | 67.5                | 42.05             | 34.78            | 28.08  | 33.36    | 23.93  |
| @t=0.0025cm [%] |                     |                   |                  |        |          |        |
| Δ               | 58.46               | 80.97             | 50.78            | 46.68  | 50.35    | 31.10  |
| @t=1.27cm [%]   |                     |                   |                  |        |          |        |
| Max             | 66.67               | 85.71             | 61.47            | 58.26  | 61.14    | 46.05  |
| @t=1.27cm [%]   |                     |                   |                  |        |          |        |
| Min             | 45.00               | 72.20             | 30.68            | 24.92  | 30.08    | 2.95   |
| @t=1.27cm [%]   |                     |                   |                  |        |          |        |
| Median          | 58.33               | 81.56             | 52.65            | 48.72  | 52.24    | 33.71  |
| @t=1.27cm [%]   |                     |                   |                  |        |          |        |

**Table 4.** Average mean relative errors [%] obtained for test case scenario 3 for both the sharp "edge" plate and the "blunt edge" plate

The comparisons between the sharp leading edges cases lead to similar results as obtained previously in test case scenario 1: the Spalding & Chi methods correlates best with the experimental data with the Smart-Meador, Monaghan and Eckert's reference temperature-based computations according to

MDAO approaches

Copyright © 2025 by author(s)

average errors. However, Poll's median error is actually lower and its range of errors much higher than all the other methods. On the flip side, Poll's formula performs the best for the bluntest edge as expected because it is meant for cylindrical shapes whereas Spalding and Chi's method performs poorly.

## 4. Methodology for the Calibration of a Reference Temperature Model

#### 4.1. Description of the Proposed Methodology

The method presented hereafter should not be regarded as a general-purpose method. With sufficient data, the approach could be generalized more broadly; however, under the present scarcity of open-source data, its applicability remains restricted. To ensure adequate performance for specific datasets or test cases, it may be necessary to calibrate a custom reference temperature-based formulation. This approach is analogous to the methodology originally proposed by Rubesin and Johnson and subsequently refined in the "SOMMER & SHORT" approach. The objective is to determine the optimal values of the constants  $K_1$  and  $K_2$  as defined by:

$$T *= T_e \times \left(1 + K_1 \times R_f \times \frac{\gamma - 1}{2} \times M_e^2 + K_2 \times \left(\frac{T_w}{T_e} - 1\right)\right) \quad (15)$$

For example, Eckert determined values of  $K_1 = 0.22$  and  $K_2 = 0.5$  based on the data he used for his parameter fitting while Poll found the following values:  $K_1 = 0.6$  and  $K_2 = 0.1$ .

In this work, a simple simulated annealing algorithm **[13]** is implemented to optimize the parameter vector  $\vec{S} = [K_1 \ K_2]$ , with the objective of minimizing the mean relative error between computed and experimental skin friction coefficients as follows:

$$TARGET = min(\Delta) = min(100 \times \langle \frac{|C_{f,DATA} - C_{f,COMPUTED}|}{C_{f,DATA}} \rangle)$$
 (16)

In this work, the choice of a Simulated Annealing algorithm-based search algorithm was based on several criteria. The first is its simplicity: it is one of the simplest metaheuristic methods one can implement in order to address a global 'black box' optimization problem. Furthermore, this algorithm is of interest as it is capable to accept transitions that can potentially degrade the objective function, meaning that we are less likely to remain trapped in a local extremum at the beginning when the value of the cooling temperature is high. Hence, it has the advantage of not being overly sensitive to its initial state. The algorithm's ability to accept an unflattering transition from a given state i to a state i+1 depends on the probability:

$$P = \begin{cases} 1 & \text{if } \Delta_{i+1} < \Delta_i \\ exp\left(\frac{\Delta_i - \Delta_{i+1}}{T_i}\right) \end{cases}$$
 (17)

The temperature  $T_i$  influences the probability of transitioning from a given state and is gradually reduced until  $T_i \cong 0$  using a cooling factor  $\alpha$ , such that  $T_i = \alpha \times T_{i-1}$ . The initial values of  $\alpha$  and  $T_0$  will influence this process. Once the cooling temperature reaches a certain residue, the search should stop. During the exploration of possible  $(K_1, K_2)$  parameters states, neighboring candidate solutions are generated by varying randomly the magnitude of the perturbations through the function f.

$$\overrightarrow{S_{i+1}} = \begin{pmatrix} K^i_1 + f(i+1) \\ K^i_2 + f(i+1) \end{pmatrix}$$

The function f simply generates a random value comprised between [-0.25, +0.25]. The random nature of the perturbation coupled with the ability of the algorithm to potentially explore unfavorable states ensures the users that the algorithm will explore the search space appropriately.

The following table recalls the hyper-parameters of interest for the upcoming studies

|                        | Description   | Value & Range considered  |  |  |
|------------------------|---|---------------------------|--|--|
| Initial<br>Temperature | Initial Temperature   | $T_0 \in \{1000,100,10\}$ |  |  |
| Alpha                  | Cooling factor  | 0.99                      |  |  |
| N                      | Maximum number of iterations  | 5000                      |  |  |
| Step size              | Maximum magnitude of the perturbations                                | +<br>-<br>-<br>0.25       |  |  |
| Acceptance criterion   | Controls the algorithms ability to transition to an unfavorable state | P (equation 18)           |  |  |
| Minimal residue        | Controls the minimal value of the cooling temperature                 | 1e-8                      |  |  |
| Search<br>Domains      | Search Spaces for values of $K_1$ , $K_2$                             | $[0.,1.] \times [0.,1.]$  |  |  |

**Table 5.** Considered Hyperparameters for section 4.2

Several constraints were considered for the implementation of this methodology. The first constraint ensures that the computed reference temperature is of a positive value:

$$K_1 \times R_f \times \frac{\gamma - 1}{2} \times M_e^2 + K_2 \times \left(\frac{T_w}{T_e} - 1\right) > -1$$
 (18)

If Condition (18) is not fulfilled, the value of  $\vec{S}$  is rejected by associating directly a disqualifying value to  $\Delta = +1000\%$ . Following this principle, a search domain is defined by taking a quick look at the 2D map of the search space where  $\Delta$  values are computed:

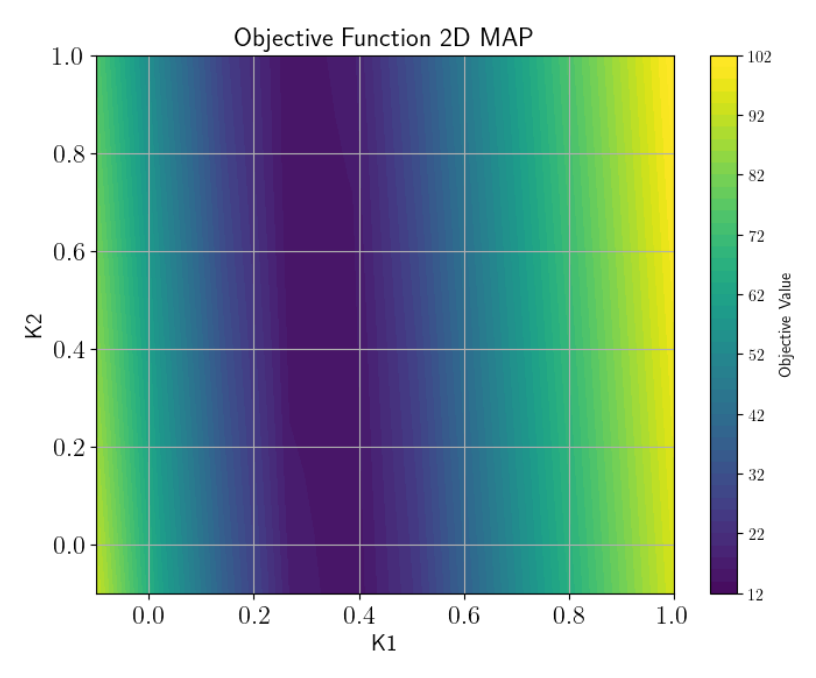


**Fig 5.** Objective Function 2D Maps where the bounding domain is represented (test case 3 @t=1.27 cm)

The previous figure highlights that there exists a large domain where solutions are unsatisfactory because condition (18) is achieved (yellow area). Furthermore, the 2D Map highlights that as values of

K1 increase, the solutions seem to become more unfavourable. Consequently, an initial bounding domain of  $[0.,1.] \times [0.,1.]$  is chosen.

### 4.2. Illustrating this methodology

A set of runs is performed for an initial state defined by Poll's constants for initial cooling temperatures:  $T \in \{1000, 100, 100\}$  for a fixed cooling factor of  $\alpha = 0.99$ . The initial state vector is initialized randomly within the bounding search space. The data set used for this illustration is the data set used in section 3.3 with a blunt leading edge of t = 1.27~cm where Poll's formula performed best with  $\Delta \sim 31\%$ . The goal of this section is to determine whether it is possible to establish a better fit for the computation of h\* for this specific configuration.

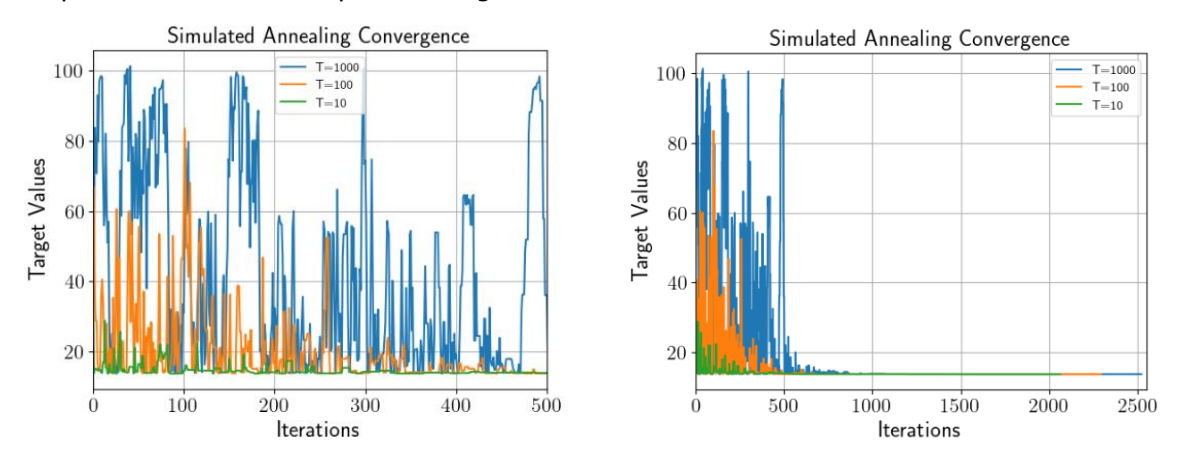


**Fig 6.** Evolution of target values  $\Delta$  [%] along the different iterations

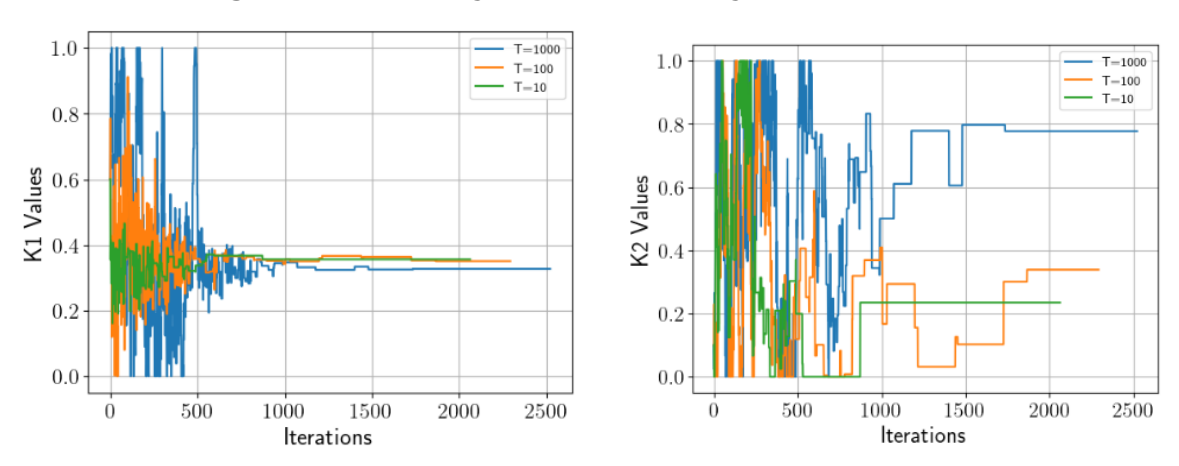


**Fig 7.** Evolution of  $K_1$  and  $K_2$  values along the different iterations

| Initial<br>Temperature | Iterations | Best ∆<br>[%] | <b>K1</b> | К2      | Median<br>[%] | Max<br>[%] | Min<br>[%] |
|------------------------|------------|---------------|-----------|---------|---------------|------------|------------|
| 1000                   | 2522       | 13.7 %        | 0.32736   | 0.77745 | 11.83         | 44.33      | 0.1        |
| 100                    | 2293       | 13.7 %        | 0.35056   | 0.33895 | 11.82         | 44.24      | 0.01       |
| 10                     | 2063       | 13.7 %        | 0.35643   | 0.23502 | 11.83         | 44.31      | 0.05       |
|                        |            |               |           |         |               |            |            |
| Poll                   |            | 31.10         | 0.6       | 0.1     | 33.71         | 46.05      | 2.95       |

**Table 6.** Results obtained for all three runs

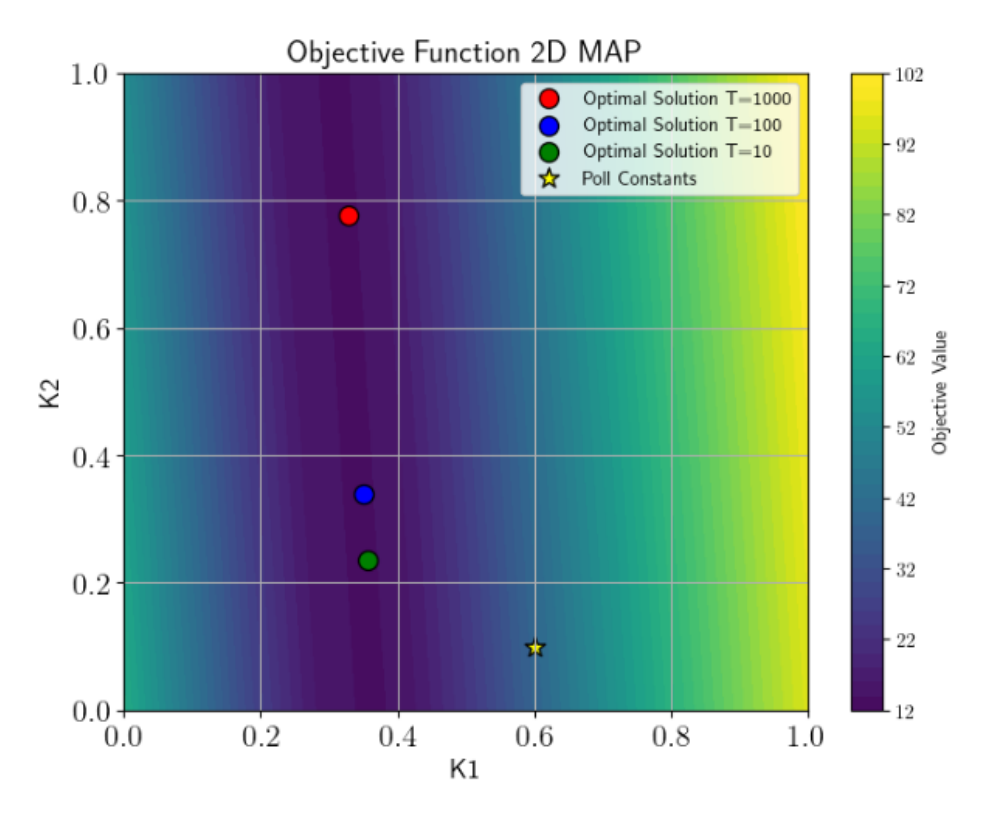


Fig 8. Target Function 2D Map with solution obtained

Three slightly different solutions are obtained thanks to the runs achieving a final mean error of  $\Delta \sim 14\%$  over the data points, which is a 17% increase in regards to Poll's function which was designed for cylindrical edges. These results highlight that for specific geometric leading-edge shapes, it is possible to adapt one's h\* computation, given access to a reliable data set. Naturally, such results are only as reliable as the validity of the dataset and are contingent on the context remaining unchanged (i.e. identical geometry).

Moreover, while all three runs lead to the same K1 value given a small uncertainty,  $K_1=0.340\pm0.022$ , the values of the K2 constants are different each run without impacting the final error value  $\Delta$ . The previous observation could be explained by the fact that the dominant term for these points is the term that is multiplied by K1, representing the contribution of the recovery factor and boundary layer edge Mach. This observation is specific to this data set and could be different assuming different conditions. Initial temperatures affect the maximum amount of iterations as the cooling process becomes faster or slower.

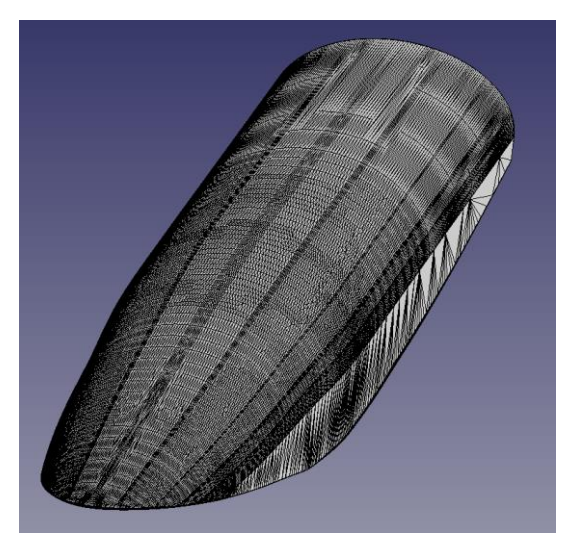
## 5. Illustrating SHAMAN's skin friction calculation procedure applicable for future MDAO loops

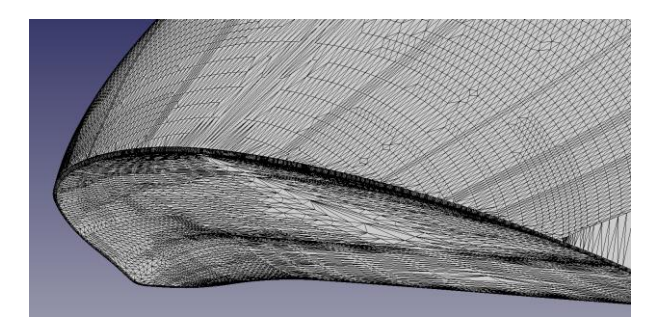
The SHAMAN software was built in order to be easily implemented with MDAO loops for rapid computations of conceptual designs. The reference temperature-based methods and the others presented in this paper can be used to rapidly compute a vehicle's friction induced drag through the estimation of its shear stress and skin friction distribution computations:

$$C_f = \frac{\tau_w}{\frac{1}{2} \times \rho_\infty \times V^2_\infty} \quad (19)$$

A brief illustration of how SHAMAN's capabilities may be applied within the context of a hypothetical MDAO loop is presented. A basic, unstructured triangulated-mesh of the ONERA hypersonic vehicle JAPHAR's main body [14] will be used as an example, as represented below:

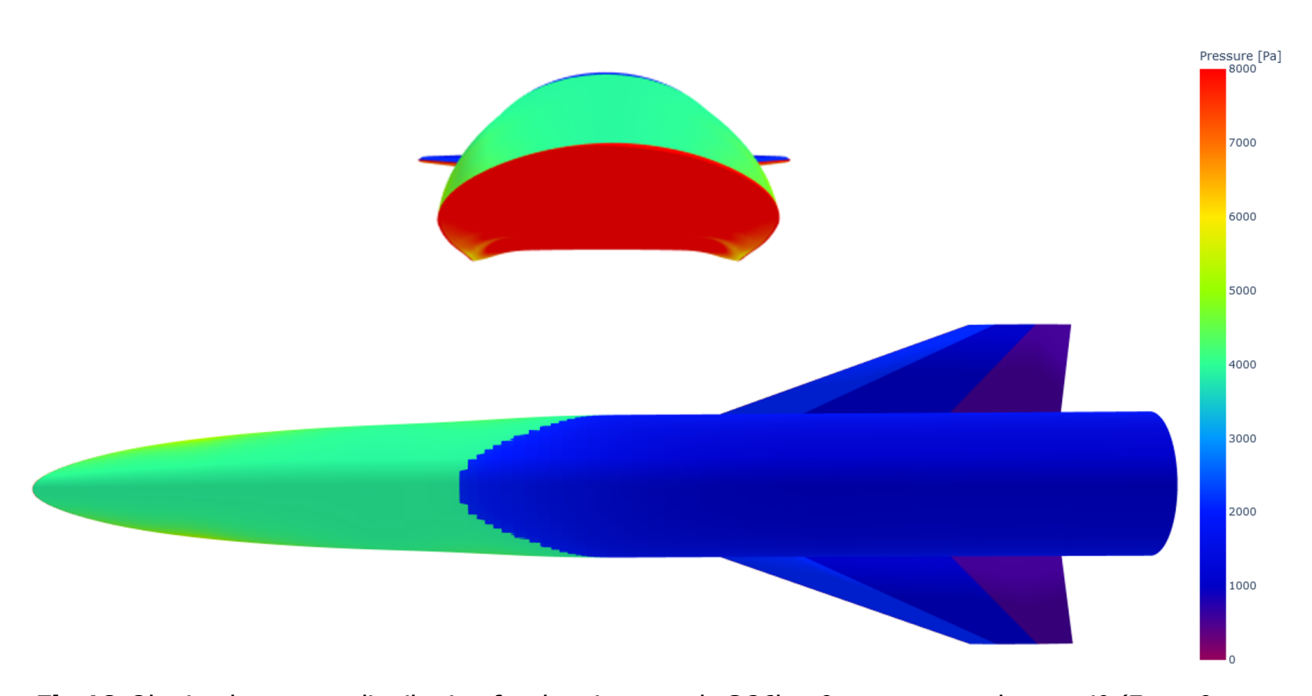
HiSST-2025-0194 Page |13
Investigation of different skin friction coefficient calculation methods applicable to the design of hypersonic vehicles using
MDAO approaches Copyright © 2025 by author(s)





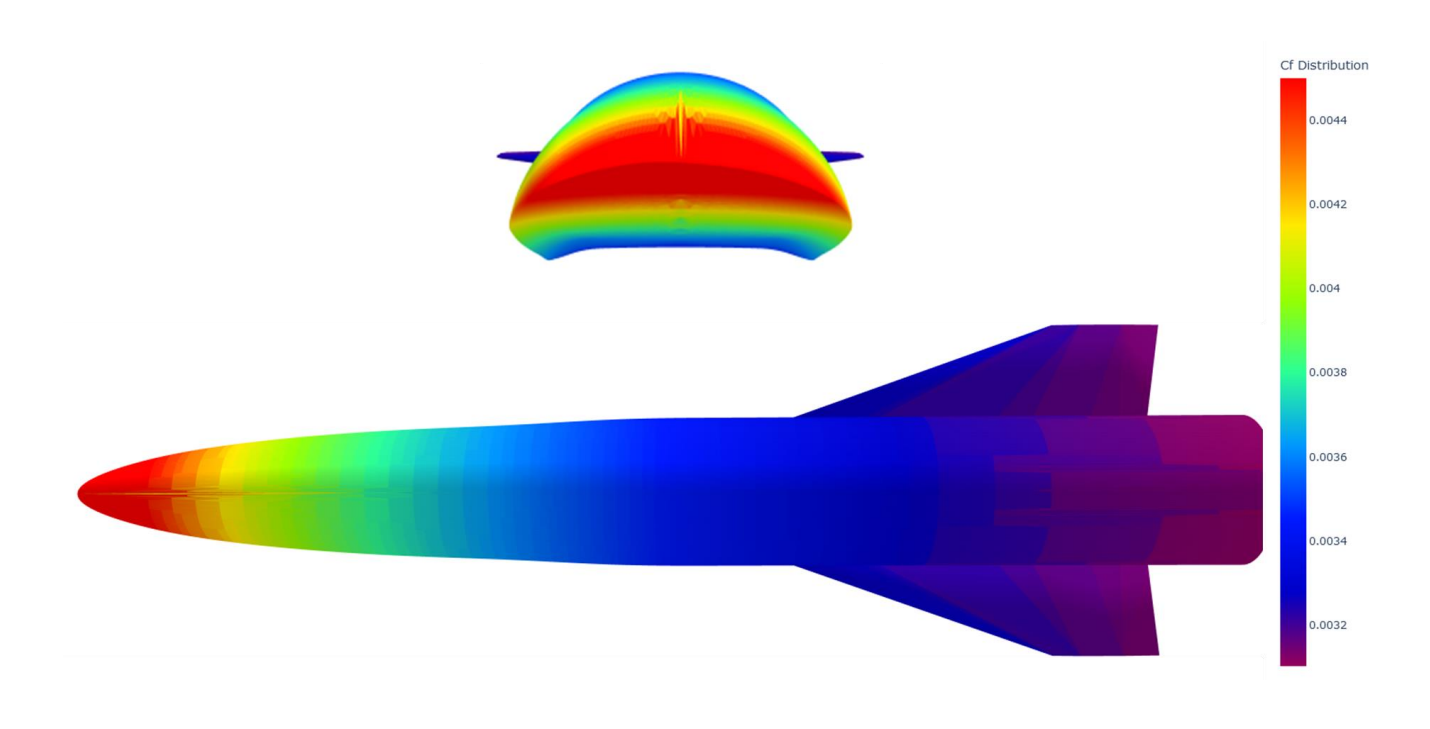
**Fig 9.** Representation of a Japhar unstructured, triangulated mesh body (FreeCAD)

The mesh represented above is comprised of a total of 55548 faces and 27780 vertices. An illustration of SHAMAN's abilities is performed on this mesh on a point at an altitude of 26 km, at Mach 7 and considering an inclination of  $+4^{\circ}$ . SHAMAN generates an atmosphere using a perfect gas ISA model and computes for each cell of the mesh an associated pressure value:



**Fig 10.** Obtained pressure distribution for the given mesh @26km &  $M_{\infty}=7$  , and a = +4° (Front & Top view)

From this pressure distribution, SHAMAN computes the associated boundary-layer edge temperature for each cell of the mesh and can compute using one of the methods presented in this paper, the associated skin friction coefficient  $C_{\rm f}$  for each cell.



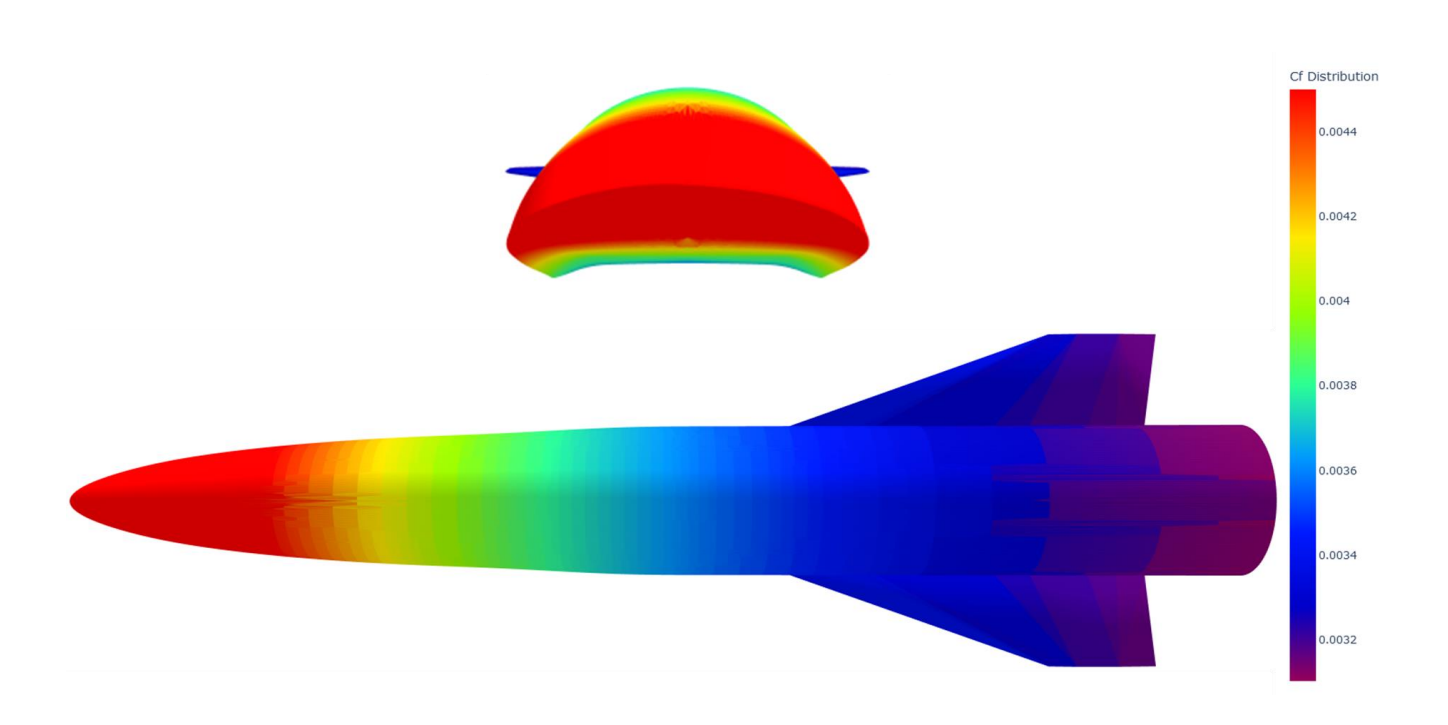


**Fig 11.** Skin friction coefficient distributions obtained using the Eckert method (Top) and the Smart-Meador method (Bottom) with Tw = 1100 K @26km &  $M_{\infty}$  = 7 , and a = +4° (Front & Top views)

#### 6. Conclusions

This paper investigates the use of different reference enthalpy-based approaches for the assessment of skin friction coefficient values in the perspective of being able to compute a vehicle's friction drag during the conceptual design, rapidly and reliably using an MDO or systems engineering approach.

The paper is mainly focused on validation works for three different test cases using open source data. The results of the first test case for the study of flat plates without pressure gradients showed that the Eckert method performed best followed closely by the Smart-Meador, Monaghan formulas and the Spalding & Chi method. Test case 2 showed that for plates that are inclined and subject to pressure gradients, a simple analytical prediction performed best. Finally, test case scenario 3 showed that when considering a blunt edged plate, Poll's method performed best. This work could be continued in future endeavors considering in-house data sets that would allow the authors to compare more accurately methods being able to monitor best uncertainties on the experimental data and their impact on the final interpretation of results. Furthermore, exploring more in-depth a scenario like test case 3 with varying bluntness thicknesses or more specific criteria for the definition of bluntness, would allow the authors to best determine when one model becomes significantly less favorable than another.

Secondly, the paper also illustrated that it is possible, using common optimization tools to better calibrate one's specific enthalpy h\* or temperature T\* formula in order to better tackle a specific geometry. This was illustrated on the blunt edged plate of test case 3, where Poll's formula performed best, being historically fitted for cylindrical edges. Future research could focus on specific test case scenarios where experimental data is collected for 'unconventional' geometries. Furthermore, the usage of symbolic regressions to do this work, that let the algorithm decide on which reference properties to mix and match to better approximate the boundary layer and thus the skin friction coefficient Cf could be explored.

Finally, SHAMAN's ability to rapidly compute pressure fields and boundary-layer properties, useful to estimate friction coefficients was shown off. Future developers and users of SHAMAN should focus on validation efforts for this aspect of the work, comparing SHAMAN's predicted skin friction coefficients with those obtained from higher fidelity CFD modelling for instance, but also, validating the integrated total skin friction drag values obtained from a rapid SHAMAN computation to a higher fidelity CFD results.

#### References

- Jack J. McNamara & Peretz P. Friedmann: 'Aeroelastic and Aerothermoelastic Analysis in Hypersonic Flow: Past, Present, and Future'. Ohio State University USA & University of Michigan USA (2012). https://arc.aiaa.org/doi/10.2514/1.J050882
- 2. G. Simeonides: 'Generalized reference enthalpy formulations and simulation of viscous effects in hypersonic flow' (1997). <a href="https://scispace.com/papers/generalized-reference-enthalpy-formulations-and-simulation-16iatubri9">https://scispace.com/papers/generalized-reference-enthalpy-formulations-and-simulation-16iatubri9</a>
- 3. Aubrey M.Cary, Jr., and Mitchel H.Bertram: "Engineering prediction of turbulent skin friction and heat transfer in high-speed flow" (1971). Nasa Langley Research Center.
- 4. J.E Wallace: "HYPERSONIC TURBULENT BOUNDARY LAYER STUDIES AT COLD WALL CONDITIONS" (1965). Aerodynamic Research Department Cornel1 Aeronautical Laboratory, Inc. Buffalo, New York.
- Edward J. Hopkins, Morris W. Rubesipz, Mumoru Inouye, Earl R. Keener, George C. Mateer, Thomus E. Pozek: "SUMMARY AND CORRELATION OF SKIN-FRICTION AND HEAT-TRANSFER DATA FOR A HYPERSONIC TURBULENT BOUNDARY LAYER ON SIMPLE SHAPES" (1967). Ames Research Center, NASA 1967
- 6. Luther NeaJ Jr: "A STUDY OF THE PRESSURE, HEAT TRANSFER, AND SKIN FRICTION ON SHARP AND BLUNT FLAT PLATES AT MACH 6.8" (1966). NASA
- 7. M.P.J Sanders: "The Boundary Layer over a Flate Plate", (2014) University of Twente
- 8. Edward J. Hopkins: "Charts for Predicting Turbulent Skin Friction from the Van Driest METHOD (II)" (1972), Technical Note, NASA Ames Research Center
- 9. B. Pearce: "A Comparison of Four Simple Calculation Methods for the Compressible Turbulent Boundary Layer on a Flat Plate" (1970), Space and Missile Systems Organization & Air Force Systems Command. Los Angeles Air Force Station California
- 10. David Aspley: "Friction Laws" (2009). University of Manchester.
- 11. Paul F. Holloway and James R. Sterrett: "Effect of controlled surface Roughness on Boundary Layer Transition and heat transfer at Mach numbers of 4.8 and 6.0". (1964) NASA, Washington D.C
- 12. Schoenherr, Karl E: "Resistance of Flat Surfaces Moving Through a Fluid" (1932), Naval Architects and Marine Engineers, volume 40
- 13. Daniel Delahey, Supatcha Chaimatanan, Marcel Mongeau: "Simulated Annealing: From basics to applications" (2018). ENAC Toulouse, France.
- 14. Ph.Novelli , W.Koschel "Progress of the JAPHAR cooperation between ONERA and DLR on hypersonic airbreathing propulsion" (2001) , ONERA and DLR
- 15. John D. Anderson Jr., "Hypersonic and High Temperature Gas Dynamics", American Institute of Aeronautics and Astronautics
- 16. Ak Sreekanth, "Aerodynamic predictive methods and their validation in hypersonic flows", Defence Research & Development Organisation Ministry of Defence, New Delhi (2003)
- 17. William E. Meador and Michael K. Smart: 'Reference Enthalpy Method Developed from Solutions of the Boundary-Layer Equations' (2005). NASA Langley Research Center, Hampton, Virginia. AAIA Journal, Volume 43.